Journal of Experimental and Theoretical Physics, Vol. 93, No. 1, 2001, pp. 188–196.
Translated from Zhurnal Éksperimental'noĭ i Teoreticheskoĭ Fiziki, Vol. 120, No. 1, 2001, pp. 214–223.

NONLINEAR PHYSICS

Big Entropy Fluctuations in Statistical Equilibrium: the Macroscopic Kinetics¶

B. V. Chirikov* and O. V. Zhirov**
Budker Institute of Nuclear Physics, Novosibirsk, 630090 Russia
**e-mail: B.V.Chirikov@inp.nsk.su*
***e-mail: zhirov@inp.nsk.su*
Received November 20, 2000

Abstract—Large entropy fluctuations in the equilibrium steady state of classical mechanics are studied in extensive numerical experiments in a simple strongly chaotic Hamiltonian model with two degrees of freedom described by the modified Arnold cat map. The rise and fall of a large separated fluctuation is shown to be described by the (regular and stable) "macroscopic" kinetics, both fast (ballistic) and slow (diffusive). We abandon a vague problem of the "appropriate" initial conditions by observing (in a long run) a spontaneous birth and death of arbitrarily big fluctuations for any initial state of our dynamical model. Statistics of the infinite chain of fluctuations similar to the Poincaré recurrences is shown to be Poissonian. A simple empirical relationship for the mean period between the fluctuations (the Poincaré "cycle") is found and confirmed in numerical experiments. We propose a new representation of the entropy via the variance of only a few trajectories ("particles") that greatly facilitates the computation and at the same time is sufficiently accurate for big fluctuations. The relation of our results to long-standing debates over the statistical "irreversibility" and the "time arrow" is briefly discussed. © *2001 MAIK "Nauka/Interperiodica".*

1. INTRODUCTION: MACROSCOPIC VERSUS MICROSCOPIC FLUCTUATIONS

Fluctuations are an inseparable part of statistical laws. This has been well known since Boltzmann. What is apparently less known are the peculiar properties of rare big fluctuations (BF) that are different from, and even in a sense opposite to, the properties of small stationary fluctuations. In this paper, we consider the simplest type of chaotic dynamical systems, namely, a Hamiltonian system with a finite number of the degrees of freedom that admits the (stable) statistical equilibrium (SE). This class of dynamical models is still popular (since Boltzmann!) in debates over the dynamical foundations of statistical mechanics (see, e.g., "Round Table on Irreversibility" in [1, 2]).

A sufficiently simple picture of BFs in such systems is well understood by now, although not yet well known. To Boltzmann, this picture was the basis of his fluctuation hypothesis for our Universe. It is also well understood that this hypothesis is totally incompatible with the present structure of the Universe because it would immediately imply the notorious "heat death" (see, e.g., [3]). For this reason, one may even term such systems the heat death models. Nevertheless, they can be and actually are widely used in describing and studying local statistical processes in thermodynamically closed systems. The latter term means the absence of any heat exchange with the environment. We note, however, that under conditions of the exponential instability of motion, which are typical of chaotic systems, the only dynamically closed system would be the "entire Universe." In particular, this excludes the hypothetical "velocity reversal" that also is popular in debates over "irreversibility" since Loschmidt (for a discussion, see, e.g., [4]).

In any case, dynamical models with the SE do not tell us the whole story of either the Universe or even a typical macroscopic process therein. The principal solution of this problem, unknown to Boltzmann, is quite clear now: the "equilibrium-free" models are required. Various classes of such models are intensively studied today. Moreover, the celebrated cosmic microwave background tells us that our Universe was born already in the state of a heat death, which, however, became unstable due to the well-known Jeans gravitational instability [5]. This resulted in developing a rich variety of collective processes, or synergetics, the term recently introduced or, better to say, put in use by Haken [6]. The most important peculiarity of such a collective instability is that the total overall relaxation (to somewhere?) with the ever increasing total entropy is accompanied by an also increasing phase space inhomogeneity of the system, particularly with respect to temperature. In other words, the entire system and its local parts become more and more nonequilibrium to the extent of the birth of a secondary dynamics that can be, and sometimes is, as perfect as, e.g., the celestial mechanics (see, e.g., [4, 7, 8] for a general discussion).

We stress that all these inhomogeneous nonequilibrium structures are not BF like in the SE but are a result

¶This article was submitted by the authors in English.

of a regular collective instability; therefore, they are immediately formed under a certain condition. In addition, they are typically dissipative structures according to Prigogine [9] due to the energy and entropy exchange with the infinite environment. The latter is the most important feature of such processes, and at the same time the main difficulty in studying the dynamics of those models both theoretically and in numerical experiments, which are so much simpler for SE systems.

In the latter case, a BF consists of two symmetric parts: the rise of a fluctuation followed by its return, or relaxation, back to the SE (see Figs. 1 and 2). Both parts are described by the same kinetic (e.g., diffusion) equation, the only difference being in the sign of time. This relates the time-symmetric dynamical equations to the time-antisymmetric kinetic (but not statistical!) equations. The principal difference between the two types of equations, sometimes overlooked, is that the kinetic equations are generally understood as describing the relaxation only, i.e., the increase of the entropy in a closed system, whereas in fact they do so (at least, in the SE) for the rise of BF as well, i.e., for the entropy decrease. All this was qualitatively known already to Boltzmann [10]. The first simple example of a symmetric BF was considered by Schrödinger [11]. A rigorous mathematical theorem for the diffusive (slow) kinetics was proved by Kolmogorov in 1937 in the paper entitled "Zur Umkehrbarkeit der statistischen Naturgesetze" (Concerning Reversibility of Statistical Laws in Nature) [12] (see also [13]). Regrettably, the principal Kolmogorov theorem still remains unknown to both the participants of heated debates over "irreversibility" and the physicists actually studying such BFs (see, e.g., [14]).

At present, there exists a well-developed ergodic theory of dynamical systems (see, e.g., [15]). In particular, it proves that the relaxation (correlation decay, or mixing) eventually proceeds in both directions of time for almost any initial conditions in a chaotic dynamical system. However, the relaxation must not always be monotonic, which simply means a BF on the way, depending on the initial conditions. To eliminate this apparently confusing (to many) "freedom," we take a different approach to the problem: instead of discussing the "true" initial conditions and/or a "necessary" restriction of them, we start our numerical experiments at arbitrary initial conditions (most likely corresponding to the SE) and observe what the dynamics and statistics of BF are like. This approach is obviously based on the fundamental hypothesis that all the statistical laws are contained in, and can be principally derived from, the underlying fundamental (Hamiltonian) dynamics. To the best of our knowledge, there is as yet no contradiction to this principal hypothesis. We note, however, that this approach can be directly applied to fluctuations in finite systems with a statistical equilibrium only (see [4] and [16] for a discussion). In these and only these systems, infinitely many BFs grow up spontaneously, independently of the initial conditions of the motion. This is similar to the well-known Poincaré recurrences (see Section 4).

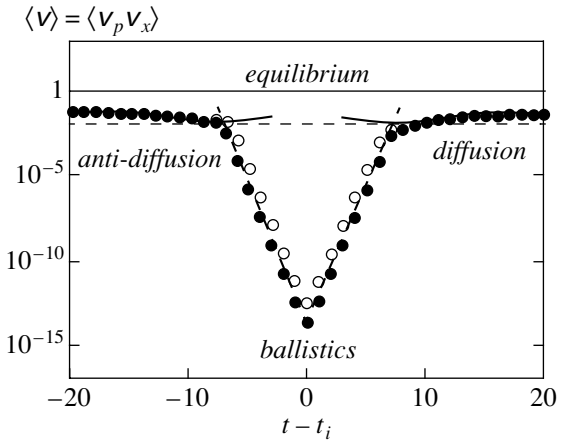

Fig. 1. Mixed kinetics for two BFs of different sizes. Filled/open circles show the time dependence of the mean variance $\langle v(t - t_i) \rangle$ around the BF maximum at $t = t_i$; the upper horizontal straight line is the equilibrium and the lower line indicates the empirical value of the dynamical scale $v_d = 0.015$, Eq. (3.4), with the parameter $F_d \approx 1/3$. The two oblique straight lines represent the expected fast kinetics, Eq. (3.3), and the two solid curves do so for the initial diffusive kinetics, Eq. (3.5). The respective run parameters and results are given by $C = 15$, $N = 1$, $v_b = 3.9 \times 10^{-11}/6.25 \times 10^{-10}$ ($v_{xb} = v_{pb}$), $v(0) = 1.96 \times 10^{-14}/3.1 \times 10^{-13}$, $n = 1971/4459$, $w = 500$. The average period between successive fluctuations is $\langle P \rangle \approx 1.4 \times 10^7/3.5 \times 10^6$ iterations.

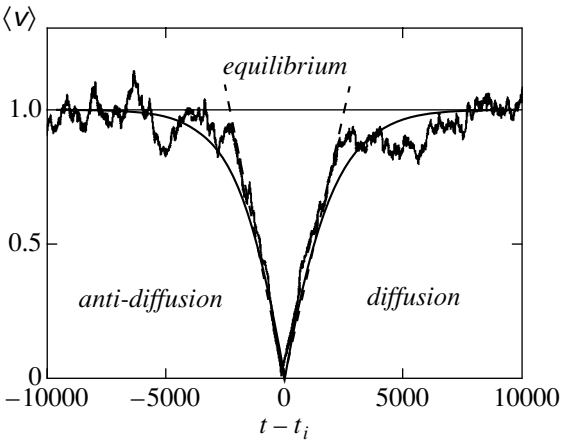

Fig. 2. The same as in Fig. 1 for a typical diffusive kinetics (anti-diffusion/diffusion): the solid curve shows the average over all $n = 20259$ fluctuations in a run and the wiggle line is the same for the first 28 fluctuations. Two oblique straight lines represent the expected initial diffusive kinetics, Eq. (3.5), with $\tau_d = 0$ and the empirical value $v_d^{(\mathrm{emp})} = 0.045$, while the theory (3.15) gives $v_d = 0.02$. Other run parameters/results are given by $C = 50$, $N = 5$, $v_b = 0.0256$, $w = 10^4$, $\langle P \rangle \approx 7.7 \times 10^5/8.7 \times 10^5$, and $B = 306/348$; $\langle P \rangle / w \approx 77/87$.

In spite of essential restrictions, simple SE models allow us to better understand the mechanism and the

role of BFs in statistical physics. In addition to the removal of the vague problem of initial conditions, these models are very helpful in clarifying the relation between macroscopic and microscopic descriptions of chaotic systems. In particular, a spontaneous rise of a BF out of the SE is a macroscopic event as well as is its subsequent relaxation back to the SE, even in a system with a few degrees of freedom. Similarly to other macroscopic processes, BFs are not only perfectly regular by themselves but also surprisingly stable against any perturbations, either regular or chaotic. Moreover, the perturbations must not be small. At a first glance, this looks very strange in a chaotic, highly unstable dynamics. The resolution of this apparent paradox is that the dynamical instability of motion affects the BF instant of time only. The BF evolution is determined by the kinetics independently of its mechanism, from a purely dynamical one, as in model (2.2) used in this paper, to a completely noisy (stochastic) one. As a matter of fact, the fundamental Kolmogorov theorem [12] is precisely related to the latter case but remains valid in a much more general situation. The surprising stability of BFs is similar to the less known concept of robustness for the Anosov (strongly chaotic) systems [17] whose trajectories are only slightly deformed under a small perturbation (see [4] for a discussion).

In this paper, we consider a particular type of BFs characterized by a large concentration of "particles" in a small phase space domain of the dynamical system. In other words, "our" fluctuations are localized in phase space and separated in time. A more accurate definition of these fluctuations is given in Section 3 (see Eq. (3.6)). The same fluctuations in a stochastic model (with noise) were studied in detail in [14]. Obviously, there exist many other fluctuations with their own peculiarities (see, e.g., [18]). The primary object of our studies is the macroscopic kinetics of big fluctuations in the background of small stationary microscopic fluctuations. A brief outline of our results was presented in [16].

2. A HAMILTONIAN MODEL: MOST SIMPLE BUT STRONGLY CHAOTIC

The systems with an SE can be described in terms of models that are very simple as regards both the theoretical analysis and numerical experiments (of which the latter are even more important for us). In the present paper, we use one of the most simple and popular models specified by the so-called Arnold cat map (see [19, 20]):

$$\begin{aligned} \bar{p} &= p + x \mod 1, \\ \bar{x} &= x + \bar{p} \mod 1, \end{aligned} \tag{2.1}$$

which is a linear canonical map on a unit torus. It has no parameters and is chaotic and even ergodic. The rate of the local exponential instability, the Lyapunov exponent $\lambda = \ln(3/2 + \sqrt{5}/2) = 0.96$, implies a fast (ballistic) kinetics with the relaxation time $t_r \sim 1/\lambda \approx 1$. Throughout the paper, t denotes the time in the map iterations.

A minor modification of this map,

$$\begin{aligned} \bar{p} &= p + x - 1/2 \mod C, \\ \bar{x} &= x + \bar{p} - C/2 \mod 1, \end{aligned} \tag{2.2}$$

where C is a circumference of the phase space torus, allows studying both the fast (exponential) ballistic kinetics (for $C = 1$) and the slow (diffusive) relaxation in p (for $C \gg 1$) with the characteristic time $t_p \sim C^2/4D_p \gg 1$, where $D_p = 1/12$ is the diffusion rate in p. In contrast to the slow diffusion in p, the relaxation time in x does not depend on C ($t_r \sim 1$) and the subsequent values of x are therefore practically uncorrelated. Map (2.2) has the (unstable) fixed point at $x = x_0 = 1/2$ and $p = p_0 = C/2$.

A convenient characteristic of the BF size is the rms volume (area) in the 2D phase space (x, p)

$$\sigma(t) = \sigma_p(t)\sigma_x(t) \tag{2.3}$$

occupied by a group of N trajectories (particles). In the ergodic motion at equilibrium, $\sigma = \sigma_0 = C/12$. Because of a severe restriction to small $N \lesssim 10$ in the numerical experiments (see below), we have to use simple (average) characteristics like (2.3) only. On the other hand, these are precisely the macroscopic variables in which we are interested.

In what follows, we also restrict ourselves to a particular case of BFs with the fixed prescribed position in the phase space,

$$x_{fl} = x_0 = \frac{1}{2}, \quad p_{fl} = p_0 = \frac{C}{2}. \tag{2.4}$$

The variance of the phase space size $v = \sigma^2 = \sigma_p^2\sigma_x^2$ is then determined by

$$\sigma_p^2 = \langle p^2 \rangle - p_0^2, \quad \sigma_x^2 = \langle x^2 \rangle - x_0^2, \tag{2.5}$$

where the brackets $\langle \ldots \rangle$ denote averaging over N trajectories. In the ergodic motion at equilibrium, $v = v_{SE} = C^2/12^2$. In what follows, we use the dimensionless measure $\tilde{v} = v/v_{SE} \longrightarrow v$ and omit the tilde. In the diffusive approximation of the kinetic equation, the variable $v(t)$ is especially convenient because it varies proportionally to time. Moreover, $v \longrightarrow v_p$ in this case because of a quick relaxation $v_x \longrightarrow 1$ in x.

Among all the advantages of v, the relation of this variable to the fundamental concept of the entropy is highly desirable. The standard definition of the entropy, which can be traced back to Boltzmann, reads

$$S = -\langle \ln f(x, p) \rangle + S_0, \tag{2.6}$$

where $f(x, p)$ is a coarse-grained distribution function, or the phase-space density, and S_0 an arbitrary constant to be fixed later. We note that the distribution calculated from any finite number of trajectories is always a

coarse-grained one. However, the direct application of Eq. (2.6) requires too many trajectories, especially for a small-size BF. Nevertheless, precisely in the latter case, which is the main problem under consideration, we have found a simple approximate relation

$$S(t) \approx \frac{1}{2}\ln v(t) \tag{2.7}$$

that gives at least a rough estimate for the entropy evolution [16]. Moreover, if the distribution is Gaussian,

$$f(x, p) \longrightarrow f(p) = \frac{\exp(-(p-p_0)^2/2v)}{\sqrt{2\pi v}}, \tag{2.8}$$

estimate (2.7) becomes exact because it is directly derived from the definition of the entropy in Eq. (2.6). The two relations for the entropy are compared in the end of Section 3 for a typical BF.

A great advantage of (2.7) is that the computation of S does not require very many trajectories as does the distribution function. In fact, even a single trajectory is sufficient, as is demonstrated by Fig. 1 in [16] and Fig. 1 in this paper!

A finite number of trajectories used for calculating the variance v is similar to a coarse-grained distribution, as required in relation (2.6), but with a free bin size that can be arbitrarily small.

We can now turn to the numerical experiments.

3. MACROSCOPIC KINETICS: COMPLETE, REGULAR, AND STABLE

In this section, we consider the regular BF kinetics. The data were obtained by simultaneously running N trajectories for a very long time in order to collect sufficiently many BFs for a reliable separation of the regular part of BFs, or the kinetic subdynamics according to Balescu (see [21] and references therein), from the stationary fluctuations. The separation was done by the plain averaging of the individual v_i values ($i = 1, \ldots, n$) over all the n BFs collected in a run.

The size of the BF chosen for the subsequent analysis is fixed by the condition that

$$v(t) < v_b \tag{3.1}$$

at some time instant $t \approx t_i$, the moment of a BF. Here, a prescribed value v_b is the main input parameter of the run. This condition actually determines the border of the entire fluctuation domain (FD) as $0 < v < v_b$.

The event of entering the FD is the macroscopic "cause" of the BF whose obvious "effect" will be the subsequent relaxation to the equilibrium. However, the main point of our study is that the second "effect" of the same "cause" was preceding the rise of the BF in an apparent contradiction with the "causality principle" (for a discussion, see [16] and Section 4 below). In any event, the second effect requires the permanent memory of trajectory segments within some time window w, which is another important input parameter of the run.

The exact procedure of data processing during the run is as follows. Starting from arbitrary (random) initial conditions, selection rule (3.1) is checked at each iteration. Suppose that it is satisfied at some instance t_{in} when the bundle of trajectories enters the FD. In the first approximation, we could consider it as the fluctuation maximum (or the variance minimum) $t_i = t_{\text{in}}$, where the subscript i is the number of the current fluctuation in a run. However, this simple procedure would cause an asymmetry with respect to $t = t_i$. A better choice would be given by the rule $t_i = (t_{\text{in}} + t_{\text{out}})/2$, where t_{out} is the time instance of the exit from the FD. Instead, we have accepted a more complicated procedure that better restores the true BF symmetry, as we hope. Starting from the moment t_{in}, we search for the minimum of $v(t)$ inside a sufficiently large interval $t_{\text{in}} < t < t_{\text{in}} + w$. If a minimum is found at some $t = t_{\min}$, we check that it also is the minimum inside the next interval $t_{\min} < t < t_{\min} + w$. If this is the case, we identify this minimum with the BF top and set $t_i = t_{\min}$; otherwise, we set $t_{\min}$ equal to the time of a better minimum and repeat the last step. Obviously, the parameter w must be small compared to $\langle P\rangle$, the mean period of the BF, but sufficiently long for the trajectory to leave FD (3.1). Typically, we chose $w \gtrsim C^2$, the total diffusion time. After fixing the current t_i value, the computation within the interval $t_i < t < t_i + w$ was completed, and only then the search for the next BF is continued.

As mentioned above, there are two quite simple limiting cases of generally very complicated kinetics, namely, the fast (ballistic) and the slow (diffusive) limits. An example of both in one run for $N = 1$ (!) is presented in Fig. 1 for two fluctuations of different sizes. In this case, general condition (3.1) was checked separately for p and x,

$$v_p(t) < v_{pb} \quad \text{and} \quad v_x(t) < v_{xb}, \tag{3.2}$$

with $v_{pb} = v_{xb} \sim 10^{-5}$ and $v_b = v_{pb}v_{xb} \sim 10^{-10}$.

The fast part of the kinetics is approximately described by

$$v(\tau) \approx v(0)\exp(4\lambda\tau), \tag{3.3}$$

where $\tau = t - t_i$, λ is the Lyapunov exponent (see Section 2) and $v(0) \sim 10^{-13}$ is the minimal variance averaged over all n fluctuations observed in the run. We note that the latter value is considerably smaller than the border value $v_b \sim 10^{-10}$. This is because of the penetration of trajectories into the FD. Interestingly, the ratio $v_b/v(0) = 2000$ is the same for both runs in Fig. 1.

A surprisingly sharp crossover to the diffusive kinetics, clearly seen in Fig. 1, is related to the dynamical scale of the diffusion corresponding to a certain size v_d of the increasing variance at which the exponential growth stops. Roughly, it occurs at the time instance

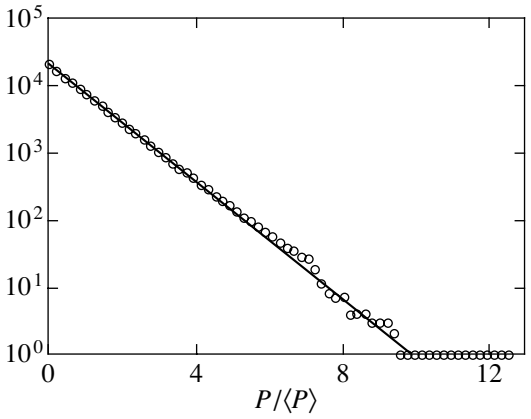

Fig. 3. The histogram of integrated distribution (3.9) for data in Fig. 2. Each circle shows the number of periods $P_m > m\Delta P$, for $m = 0, 1, \ldots$ $P_0 = n$, $\Delta P = 1.5 \times 10^5$; $P_{\min}/w = 1.0027$; $P_{\max}/\langle P\rangle = 12.63$; $\langle P\rangle = 765084$. The straight line is the expected distribution $n\exp(-P/\langle P\rangle)$.

$\tau = \tau_d$, when $|x - x_0| \sim |p - p_0| \sim 1/2$, whence $\nu_{xd} \sim 12/4 = 3$ and $\nu_{pd} \sim 3/C^2$. We can therefore characterize the dynamical scale as

$$\nu(\tau_d) = \nu_d = F_d \nu_{pd} \nu_{xd} = \frac{9F_d}{C^2}, \qquad \tau_d = \frac{\ln(\nu_d/\nu(0))}{4\lambda}, \tag{3.4}$$

where F_d is an empirical factor and τ_d is found from Eq. (3.3). The data in Fig. 1 imply the dynamical scale $\nu_d \approx 0.015$ independently of ν_b, which gives the empirical factor $F_d \approx 1/3$.

In the diffusion region ($\nu > \nu_d$), the initial kinetics is described by a simple relation for the free diffusion (see Section 2),

$$\nu(\tau) \approx \frac{\tau \pm \tau_d}{C^2} + \nu_d, \quad \tau_d < \tau \ll C^2, \tag{3.5}$$

which is also shown in Fig. 1. It involves two corrections, τ_d and ν_d, due to the exponential ballistic kinetics. The first one (with opposite signs for the two symmetric parts of the fluctuation) takes the "lost" time after (or prior to) the antidiffusion (diffusion) into account, while the second correction describes a finite fluctuation size at the crossover from (to) the diffusion. The mean empirical value $\tau_d = 7$ used in Fig. 1 is close to the value $\tau_d = 6.5$ found from Eq. (3.4) with another empirical quantity, $\nu_d = 0.015$.

The large ratio

$$B = \frac{\langle P\rangle}{C^2} \gg 1 \tag{3.6}$$

of the mean fluctuation period $\langle P\rangle$ to the characteristic time of the diffusion relaxation (see Eq. (3.5)) is the definition of a big fluctuation. It guarantees the time separation of successive fluctuations.

We now turn to the main subject of our study, the purely diffusive kinetics of BFs. For this, we first eliminate the x-statistics by excluding ν_x from selection condition (3.1), which now reads

$$\nu(t) = \nu_p < \nu_{pb} = \nu_b. \tag{3.7}$$

Next, the variance ν_b must now exceed the new dynamical border,

$$\nu_b > \nu_d = \nu_{pd} \approx f_p \frac{12}{C^2} \tag{3.8}$$

with some empirical factor $f_p \approx 1$ (see Eq. (3.4) and the discussion below).

A typical example of a diffusive BF is shown in Fig. 2. Both the regular macroscopic kinetics of the antidiffusion/diffusion and the irregular fluctuations around are clearly seen. We note that their size rapidly decreases toward the BF maximum. It may even seem that the motion becomes regular in that region, hence the term "optimal fluctuational path" [14]. In fact, the motion remains diffusive down to the dynamical scale $\nu \sim \nu_d$ in Eq. (3.8).

Even though a separate BF is sufficiently regular, the time instance of its spontaneous appearance t_i and, hence, the individual period P are random in the chaotic system. Due to the statistical independence of BFs under condition (3.6), the expected distribution in P is Poissonian (Fig. 3),

$$f(P) = \frac{\exp(-P/\langle P\rangle)}{\langle P\rangle}. \tag{3.9}$$

The principal characteristic of the period statistics, $\langle P\rangle$, can be estimated as follows. From the ergodicity of motion in the N-dimensional momentum space, we have

$$\Phi = \frac{T_s}{t_f} = \frac{\langle T_s\rangle}{\langle P\rangle} = \frac{\mathcal{P}_{fl}}{\mathcal{P}_{eq}}. \tag{3.10}$$

This is an exact relation (in the limit as $t_{\rm run} \longrightarrow \infty$), with T_s being the total sojourn time of trajectories within the FD (under the condition $\nu(t) < \nu_b$) during the entire run time $t_{\rm run}$ and $\langle T_s\rangle$ the same per fluctuation. Both ratios are equal to the ratio of the N-dimensional momentum volume $\mathcal{P}$ of the fluctuation at $\tau = 0$ to that in the equilibrium. The ratio Φ was also measured during the run. It follows that

$$\langle P\rangle = \frac{\langle T_s\rangle}{\Phi}. \tag{3.11}$$

The next, more difficult step is the valuation of $T_s = 2T_{\rm ex}$ from the diffusion equation, where $T_{\rm ex}$ is the exit (or entrance due to symmetry) time from (or to) the FD.

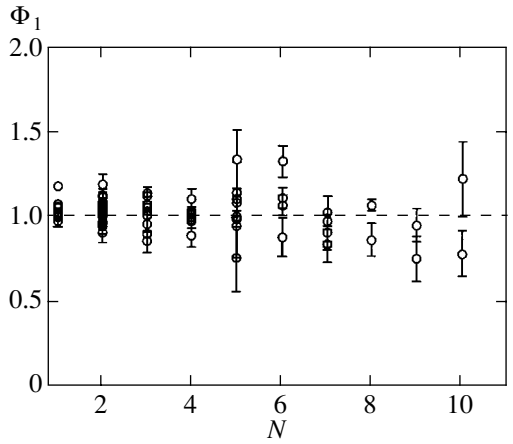

Fig. 4. The comparison of the directly measured ratio Φ_{emp} given by Eq. (3.10) with the theoretical approximation Φ_{th}, Eq. (3.12) for $N = 1$–10: $\Phi_1 = \Phi_{emp}/\Phi_{th}$; the average over 71 runs is $\langle\Phi_1\rangle = 1.015 \pm 0.11$ (the standard deviation); the bars show statistical errors $1/\sqrt{n}$ for each run; the total number of fluctuations in all runs is 127346.

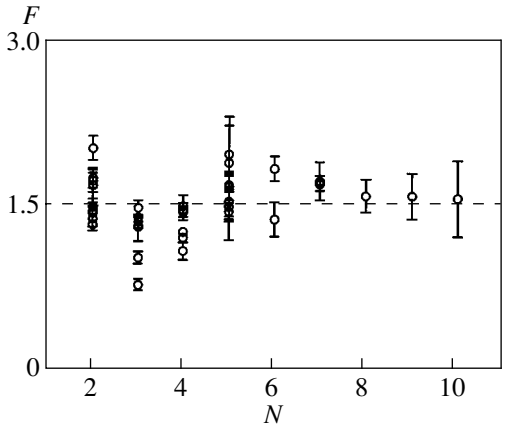

Fig. 5. The comparison of the empirical data for 36 runs selected from 61 runs computed for $N = 2$–10 by the two rules, Eq. (3.6) with $B > 7$ and Eq. (3.15) with $A = 6$, to theoretical relation (3.14) with the main fitting factor F_m, $m = 1, \ldots, 36$ (see text). The average value is $\langle F\rangle = 1.51(1 \pm 0.17)$ (the standard deviation); the bars show statistical errors $F_m/\sqrt{n}$ for each run; the total number of fluctuations in 36 runs is 34429.

A simple crude estimate is $T_{ex} \sim \nu_b/D_p = \nu_b C^2$ (see Section 2). However, the first numerical experiments have already revealed that the actual exit time is much shorter, roughly by the factor $1/N^2$. A plausible explanation is that inside the FD, the distribution is concentrated in a relatively narrow layer at the surface of the N-dimensional sphere determined by the selection condition $\nu(t) < \nu_b$ in Eq. (3.7). The relative width of the layer $\sim 1/N$ then implies the observed factor $\sim 1/N^2$. Further, the ratio

$$\Phi(\nu_b, N) = \nu_b^{N/2}\phi(N), \tag{3.12}$$

with the geometrical function

$$\phi(N) \approx \left(\frac{\pi e}{6}\right)^{N/2}\frac{(1 - 1/6N)}{\sqrt{\pi N}}, \tag{3.13}$$

admits a relatively accurate approximation down to $N = 1$ (see Fig. 4).

Collecting all the above formulas, we arrive at our final empirical relation

$$\langle P\rangle \approx \frac{F}{\Phi}\frac{2\nu_b AC^2}{N^2} \approx F\frac{2AC^2}{N^2}\frac{\nu_b^{1-N/2}}{\phi(N)} \tag{3.14}$$

with two fitting factors, A for the layer width and F for all the other approximations made above. The two factors cannot be united in one because the former enters a new expression for the dynamical scale that naturally generalizes Eq. (3.8). Together with inequality (3.6) for a big fluctuation, the new dynamical scale was used in selecting purely diffusive BFs described by Eq. (3.14). The corresponding inequality reads (cf. Eq. (3.8))

$$\nu_b > \nu_d, \quad \nu_d\frac{A}{N^2} \approx f_p\frac{12}{C^2}, \tag{3.15}$$

which means that even a small part ($A/N^2 < 1$) of the FD must exceed the dynamical scale.

All the empirical parameters were optimized as follows. The values of two factors, B in Eq. (3.6) and f_p in (3.15), are not crucial; larger values of these factors correspond to a better selection of purely diffusive BF but reduce the amount of the empirical data available. A compromise was found at $B = 7$ and $f_p = 1$, which leaves 36 runs of 61 done and 34429 of the total 75053 BFs computed with $N = 2$–10 for comparison to Eq. (3.14). This was executed as follows. For each selected run with the parameters N, C, and ν_b and the computed values $\langle P\rangle$ and Φ, the empirical factor F (which was assumed to be a constant) was calculated from the first equation in (3.14). The value of A was chosen by minimizing the relative standard deviation to $\Delta F/\langle F\rangle = 0.17$. For a given set of data, the result was $A \approx 6$. The final dependence $F(N)$ is shown in Fig. 5, where the bars are the statistical errors $F/\sqrt{n}$ for each run.

Coming to the analysis of our main theoretical result, the second equation in (3.14), we first remark that it does not describe a single trajectory ($N = 1$). This is because we excluded ν_{xb} from selection condition (3.7) (cf. Eq. (3.2)) and thus reduced the phase space dimension to the minimal value, unity. In this case, a single trajectory repeatedly crosses the FD with the period $P \sim C^2$, the entire diffusion time around the phase space torus, which is independent of the FD size.

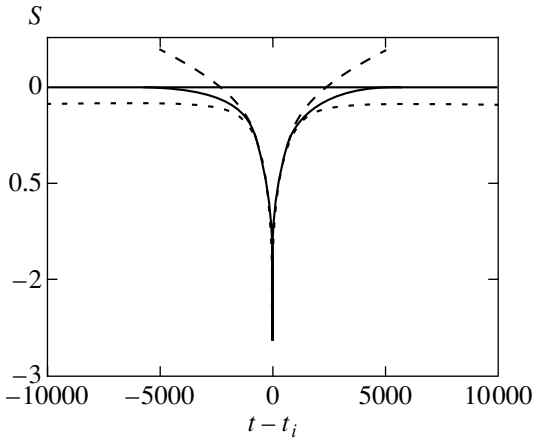

Fig. 6. The macroscopic kinetics of the BF entropy: the lower line is the "exact" entropy given by Eq. (2.6), to be compared with approximation (2.7), the middle line; the upper line is the same approximation for the diffusion theory, Eq. (3.5) with $\tau_d = 0$ and the empirical value $\nu_d^{(\mathrm{emp})} = 0.02$. The run parameters/results are $C = 50$, $N = 5$, $\nu_b = 0.01$, $w = 10^4$, $n = 4580$, $\langle P\rangle \approx 3.3 \times 10^6$, $B = 1314$; $\langle P\rangle/w \approx 329$. The number of partition bins for calculating (2.6) is $N_p = 401$.

More formally, this also follows from Eq. (3.14), because condition (3.6) cannot be satisfied for small ν_b.

For two trajectories ($N = 2$), the period does not depend on ν_b, and for the data in Fig. 5, we have the ratio $\langle P\rangle/C^2 \approx 8.7$. Because of fluctuations, the actual values of this ratio are in the interval 7.4–11.0, still not too big for a BF. Apparently, this leads to a relatively large scattering of points with $N = 2$, which also persists for $N = 3$.

The main dependence in Eq. (3.14), the exponential of N, is readily derived from a graphic picture of N statistically independent particles gathering together inside a small domain with the probability $\sim 1/P \sim \nu_b^{N/2}$. Such estimates are known for the Poincaré recurrences since Boltzmann [10]. The estimate is especially vivid in the geometrical picture of the N-dimensional sphere of the radius $\sqrt{\nu_b}$ considered above. Our empirical relation (3.14) considerably improves the simple estimate by including a weaker power-law dependence, which is evident in Fig. 5.

In our studies described above, we fixed the position of a BF in phase space, Eq. (2.4). If we lift this restriction, the probability of a BF increases by the factor $\nu_b^{-1/2}$, which corresponds to decreasing N by one ($N \longrightarrow N - 1$) because only $N - 1$ trajectories then remain independent. With the latter change, all the above relations presumably remain valid.

Our main relation (3.14) describes the diffusive kinetics for $\nu_b > \nu_d$, Eq. (3.15), when a BF is not too big. In the opposite case $\nu_b \ll \nu_d$ of a very big fluctuation, as in Fig. 1, the dependence $\langle P(\nu_b)\rangle$ becomes much simpler (see Eqs. (3.11)–(3.13) and [16]):

$$\langle P(\nu_b)\rangle = \frac{\langle T_s\rangle}{\Phi} \approx \frac{2}{\nu_b^{N/2}\phi(N)} \approx 2\nu_b^{-N/2}. \qquad (3.16)$$

This is explained by a fast exponential kinetics near the BF top (Fig. 1), which implies the shortest exit time $T_{\mathrm{ex}} \approx 1$, and hence, $T_s \approx 2$. Indeed, for both BFs in Fig. 1, we have the empirical value $\langle P\rangle\Phi = 1.98$.

In the conclusion of this section, we show in Fig. 6 the macroscopic kinetics of the BF entropy, both the "exact" one in Eq. (2.6), calculated for the partition of the entire interval ($0 < p < C$) into $N_p = 401$ bins, and the one given by our approximation (2.7). Both entropies were calculated for the same 5 trajectories in one run. The necessary statistics for the exact entropy was obtained at the expense of a large number $n = 4580$ of fluctuations in the run. To compare the two entropies, we must adjust the constant S_0 in Eq. (2.6). As is easily verified, Gaussian distribution (2.8) leads exactly to relation (2.7) if

$$S_0 = -\frac{1}{2}\ln(2\pi e) \approx -1.4189 \approx -\sqrt{2}. \qquad (3.17)$$

Approximation (2.7) is valid for the most part of the BF except a relatively small domain near the equilibrium, where the distribution in p approaches the homogeneous one. The exact entropy (with constant (3.17)) in the equilibrium is

$$S_{SE} = -\frac{1}{2}\ln\left(\frac{\pi e}{6}\right) \approx -0.18 \qquad (3.18)$$

instead of zero in approximation (2.7). The difference is relatively small, the larger the fluctuation. In the main part of the BF, our simple relation for the entropy in Eq. (2.7) reproduces exact relation (2.6) to a surprisingly good accuracy. This confirms that the distribution in p is indeed very close to the Gaussian one in Eq. (2.8), as expected.

4. CONCLUSION: THERMODYNAMIC ARROW?

We have presented the results of extensive numerical experiments on big entropy fluctuations (BFs) in a statistical equilibrium (SE) of classical dynamical systems and discussed their peculiarities.

All numerical experiments were carried out on the basis of a very simple model given by Arnold cat map (2.1) on a unit torus with only two minor, but important and helpful, modifications:

(1) expanding the torus in the p direction, Eq. (2.2), for a more impressive diffusive kinetics of BFs out of the equilibrium (Fig. 2), and

(2) inserting a special (unstable) fixed point for a better demonstration of the exponential ballistic kinet-

ics (Fig. 1). In addition, this point was used as a fixed position of BFs, which relates our studies of BFs to another interesting and important problem, the Poincaré recurrences (see Eq. (2.2)).

The most important distinction of our approach is that we have abandoned the vague question of the initial conditions, in particular, a "necessary" restriction of those in statistical physics. Instead, we started our numerical experiments at arbitrary initial conditions (most likely corresponding to the SE), and did observe the dynamics and statistics of BFs. In other words, we studied the spontaneous BFs only.

It is also important that such a spontaneous rise of a BF out of the SE and its subsequent relaxation back to the SE can be considered as a statistical macroscopic event, even in a system with a few degrees of freedom as the one in Eq. (2.2). The term "macroscopic" refers to average quantities including variance, entropy, mean period, distribution function, and the like.

We consider a particular class of BFs that we call the Boltzmann fluctuations. They are obviously symmetric under the time reversal (see Figs. 1, 2, and 6), and therefore, at least in this case, there is no physical reason at all for the concept of the notorious "time arrow." Nevertheless, a related concept—the *thermodynamic* arrow pointing in the direction of the average increase of entropy—makes sense in spite of the time symmetry [16]. The point is that the BF characteristic relaxation time is determined by the model parameter C only and does not depend on the BF itself. On the contrary, the expectation time for a given BF, or the mean period between successive fluctuations, rapidly grows with the BF size and with the number of trajectories (or the degrees of freedom), Eq. (3.14). A large ratio of the two quantities, $B = \langle P\rangle/C^2 \gg 1$, is our definition of a big fluctuation, Eq. (3.6). A similar result was recently obtained in [22], but the authors missed the principal difference between the time arrow and the thermodynamic arrow.

A related notion of the causality arrow, which by definition points from an independent macroscopic cause to its effect, also makes some physical sense (see [16] and Section 3 for a discussion). For the Boltzmann BFs considered in the present paper, the directions of both arrows coincide independently of the direction of time. In our opinion, the last statement is the most important, philosophical "moral" that the principally well-known Boltzmann fluctuations teach us.

Even though we discuss and interpret our empirical results in terms of entropy (S), which is the most fundamental concept in statistical physics, we actually use another entropy-like quantity, the variance $\nu(t)$ for a group of N trajectories, Eq. (2.5). One reason is technical: the computation of ν is much simpler than that of $S(t)$, which is either very time-consuming in numerical experiments (for exact S given by (2.6)) or approximate in accordance with (2.7). In addition, for diffusive kinetics, in which we are mainly interested, the variance is a natural variable that makes the BF picture most simple and comprehensible.

Originally, we planned to cover both sides of the BF phenomenon, the regular macroscopic kinetics and the accompanying microscopic fluctuations (noise) around. However, our numerical experiments revealed a much more complicated structure of the latter, as an example in Fig. 2 demonstrates. The dependence $\nu(t)$ looks like a fractal curve on a variety of time scales, ranging from the minimal one ~1 iteration up to $\sim C^2$, which is comparable to that of the BF itself. This interesting problem certainly requires and deserves further studies.

Only the fluctuations in classical mechanics are considered in this paper. General quantum fluctuations are quite different. However, according to the Correspondence Principle, the dynamics and statistics of a quantum system in the semiclassical region are close to the classical ones at the appropriate time scales, the longest of which corresponds to the diffusive kinetics and ensures the transition to the classical limit (see [4, 23] for details). Curiously, the computer classical dynamics that is the simulation of a classical dynamical system on digital computer is of a qualitatively similar character. This is because any quantity is discrete ("overquantized") in the computer representation. As a result, the correspondence between the classical continuous dynamics and its computer representation in numerical experiments is generally restricted to certain finite time scales as in quantum mechanics (see the first two references in [23]).

The discreteness of the computer phase space leads to another peculiar phenomenon: generally, the computer dynamics is irreversible due to the rounding-off operation unless a special algorithm is used in numerical experiments. However, this does not affect the statistical properties of the chaotic computer dynamics. In particular, the statistical laws remain time-reversible in the computer representation in spite of the (nondissipative) irreversibility of the underlying dynamics. This simple example demonstrates that contrary to a common belief, the statistical reversibility is a more general property than the dynamical reversibility.

REFERENCES

1. J. Lebowitz, I. Prigogine, and D. Ruelle, Physica A (Amsterdam) **263**, 516 (1999).
2. J. Lebowitz, Physica A (Amsterdam) **194**, 1 (1993).
3. L. D. Landau and E. M. Lifshitz, *Statistical Physics* (Nauka, Moscow, 1995; Pergamon, Oxford, 1980), Part 1.
4. B. V. Chirikov, in *Law and Prediction in the Light of Chaos Research*, Ed. by P. Weingartner and G. Schurz (Springer-Verlag, Berlin, 1996), p. 10; Open Systems and Information Dynamics **4**, 241 (1997); chao-dyn/9705003 (1997); Wiss. Z. Humboldt-Univ. Berl., Ges.-Sprachwiss. Reihe **24**, 215 (1975).
5. J. Jeans, Philos. Trans. R. Soc. London, Ser. A **199**, 1 (1929).

6. H. Haken, *Synergetics: an Introduction* (Springer-Verlag, Berlin, 1978; Mir, Moscow, 1980).
7. A. Turing, Philos. Trans. R. Soc. London, Ser. B **237**, 37 (1952); G. Nicolis and I. Prigogine, *Self-Organization in Non-Equilibrium Systems* (Wiley, New York, 1977; Mir, Moscow, 1979).
8. A. Cottrell, in *The Encyclopedia of Ignorance*, Ed. by R. Duncan and M. Weston-Smith (Pergamon, Oxford, 1977), p. 129.
9. P. Glansdorf and I. Prigogine, *Thermodynamic Theory of Structure, Stability, and Fluctuations* (Wiley, New York, 1971; Mir, Moscow, 1972).
10. L. Boltzmann, *Vorlesungen über Gastheorie* (J. A. Barth, Leipzig, 1896-98; Gostekhizdat, Moscow, 1956); *Lectures on Gas Theory* (Univ. of California Press, Berkeley, 1964).
11. E. Schrödinger, *Über die Umkehrung der Naturgesetze* (Sitzungsber. Preuss. Akad. Wiss., 1931), p. 144.
12. A. N. Kolmogoroff, Math. Ann. **112,** 155 (1936); **113**, 766 (1937).
13. A. M. Yaglom, Dokl. Akad. Nauk SSSR **56**, 347 (1947); Mat. Sb. **24**, 457 (1949).
14. D. G. Luchinsky, P. McKlintock, and M. I. Dykman, Rep. Prog. Phys. **61**, 889 (1998).
15. I. P. Kornfel'd, Ya. G. Sinaĭ, and S. V. Fomin, *The Theory of Ergodicity* (Nauka, Moscow, 1980).
16. B. V. Chirikov, Zh. Éksp. Teor. Fiz. **119**, 205 (2001) [JETP **92**, 179 (2001)].
17. D. V. Anosov, Dokl. Akad. Nauk SSSR **145**, 707 (1962).
18. L. Schulman, Phys. Rev. Lett. **83**, 5419 (1999); G. Casati, B. V. Chirikov, and O. V. Zhirov, Phys. Rev. Lett. **85**, 896 (2000); D. Evans, D. Searles, and E. Mittag, cond-mat/0008421 (2000); B. V. Chirikov and O. V. Zhirov, cond-mat/0009125 (2000).
19. V. I. Arnold and A. Avez, *Ergodic Problems of Classical Mechanics* (Benjamin, New York, 1968; Izhevsk, 1999).
20. A. J. Lichtenberg and M. A. Lieberman, *Regular and Stochastic Dynamics* (Springer-Verlag, New York, 1992).
21. R. Balescu, *Equilibrium and Nonequilibrium Statistical Mechanics* (Wiley, New York, 1975; Mir, Moscow, 1978).
22. R. Metzler, W. Kinzel, and I. Kanter, cond-mat/0007382 (2000).
23. B. V. Chirikov, F. M. Izrailev, and D. L. Shepelyansky, Sov. Sci. Rev., Sect. C **2**, 209 (1981); B. V. Chirikov, in *Lectures in Les Houches Summer School on Chaos and Quantum Physics, 1989* (Elsevier, Amsterdam, 1991), p. 443; G. Casati and B. V. Chirikov, in *Quantum Chaos: Between Order and Disorder*, Ed. by G. Casati and B. V. Chirikov (Cambridge Univ. Press, Cambridge, 1995), p. 3; Physica D (Amsterdam) **86**, 220 (1995); B. V. Chirikov, in *Proceedings of the International Conference on Nonlinear Dynamics, Chaotic and Complex Systems*, Zakopane, 1995, Ed. by E. Infeld, R. Zelazny, and A. Galkowski (Cambridge Univ. Press, Cambridge, 1997), p. 149; B. V. Chirikov and F. Vivaldi, Physica D (Amsterdam) **129**, 223 (1999).